

DesignCon 2010

A New Crosstalk Jitter Separation Method

Mike Li, Daniel Chow, and Masashi Shimanouchi

Altera Corporation

Abstract

We have developed a new crosstalk jitter (XJ) separation method and algorithm that separates crosstalk jitter from the rest of the jitter components. Finally, this long-standing problem confronting the modern jitter field has received a proven and verified solution. The method presented in this paper classifies XJ into two types, correlated crosstalk jitter (CXJ) and uncorrelated crosstalk jitter (UXJ), and separates them according to their distinct characteristics. The feasibility and validity of this new crosstalk jitter separation is further demonstrated and proven with controlled experiments.

Author Biography

Dr. Mike Peng Li

As a principle architecture and distinguished engineer at Altera Corporation, Dr. Mike Peng Li is a corporate expert and adviser on jitter, noise, and high-speed link and SERDES architecture. Dr. Li pioneered a jitter separation method (Tailfit); DJ, RJ, and TJ concept and theory formation; and jitter transfer function (JTF) concept, theory, and application for high-speed serial link design analysis and validation. He is involved in setting and contributing to standards for jitter, noise, and signal integrity for leading serial data communications, such as Fibre Channel, Gigabit Ethernet, Serial ATA, PCI Express, and FB DIMM. Currently, he is co-chairman of the PCI Express jitter standard committee. Dr. Li has been involved in and led technical committees for IEEE- and IEC-sponsored technical conferences, such as Custom Integrated Circuits Conference (CICC), International Test Conference (ITC), and DesignCon, and is a constant speaker, invited author, panelist, and session and panel chair on the subjects of jitter, noise, and signal integrity covering both design and test.

Prior to joining Altera in 2007, Dr. Li was the chief technology officer (CTO) at Wavecrest Corporation, where he developed the technology leadership and vision for the company. He has received many awards, including design paper awards from DesignCon and IEC and contribution awards from PCI-SIG. He has been listed in *Who's Who in America* and *Who's Who in the World* since 2006. Dr. Li has authored or co-authored five books and book chapters on jitter and high-speed I/O, including the widely distributed and highly ranked book *Jitter, Noise, and Signal Integrity at High-Speed*. He has published more than 80 technical papers, and holds six patents with 12 pending. Dr. Li holds a PhD in physics, an MSE in electrical and computer engineering, and an MS in physics, all from the University of Alabama, Huntsville. He also holds a BS in physics from the University of Science and Technology of China. He did his post-doctoral work at University of California, Berkeley, where he worked as a high-energy astrophysicist before joining the industry.

Dr. Daniel Chow

Dr. Chow is a senior member of technical staff at Altera Corporation. His responsibilities include defining testing and validation methodologies of high-speed components. Specifically, he is responsible for developing Altera's knowledge base on jitter measurement issues. Dr. Chow received his PhD from the University of California, Davis.

Mr. Masashi Shimanouchi

Mr. Shimanouchi is a senior member of technical staff at Altera Corporation. His work on the high-speed serial links in FPGA products includes link system and component architecture, modeling, characterization, and link jitter and BER simulation tools development with expertise in the signal integrity and jitter area. He has over 20 years experience in the R&D of test and measurement instrumentation products ranging from high-speed ATEs to oil exploration instruments. Prior to joining Altera in 2008, he was a senior staff engineer at Credence/NPTest/Schlumberger in charge of the signal integrity and timing accuracy of high-speed ATEs. He has published four technical papers and holds three patents. He holds a BS degree in physics from Keio University in Tokyo, Japan.

1. Introduction

As the data rate for high-speed serial communication continues to increase, reaching 10 Gbps and beyond, the unit interval (UI) keeps decreasing and every jitter component for the link must be shrunk or compensated to maintain the same bit error rate (BER). To meet this ever-challenging requirement, theories and quantification methods for every jitter component or root cause must be in place or be developed.

In the past 10 years, significant research and development efforts have been spent on understanding jitter and methodologies for jitter component separation (e.g., [1], [2], [3], [4], [5]). It is well acknowledged and understood that jitter has deterministic jitter (DJ) and random jitter (RJ) components at the first layer separation. DJ includes data-dependent jitter (DDJ), periodic jitter (PJ), and bounded un-correlated jitter (BUJ) sub-components, and DDJ includes intersymbol interference (ISI) and duty cycle distortion (DCD) sub-components. This jitter component hierarchy is illustrated in Figure 1.

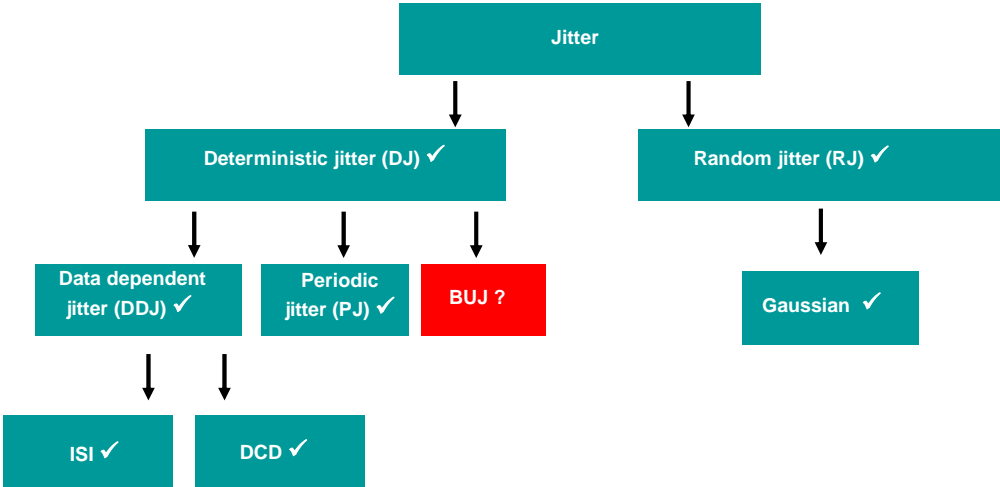


Figure 1. A jitter component hierarchy

There has been little or no development of the BUJ separation theory and methodology compared with that for other jitter components. BUJ terminology was first created by Fibre Channel T11 committee [6] to capture and cover all the uncorrelated jitter components, including uncorrelated crosstalk jitter and uncorrelated interferences. As yet, no formal papers in publicly available technical conferences or journals discuss how to separate crosstalk jitter from the rest of jitter components. Thus, the BUJ, or more specifically, the crosstalk-jitter separation method, along with its validity and accuracy, is still relatively unknown.

On the other hand, crosstalk as a physical phenomenon and mechanism has been studied across a wide range of fields, such as chip-level crosstalk (e.g., crosstalk for VLSI interconnects, and crosstalk for package), and board-level crosstalk. In the field of high-speed serial link with multiple lanes, crosstalk is an important topic, especially when the data rate approaches 10 Gbps and beyond. Because XJ is not compensated by most equalizations, it must be reduced or well bounded to insure the interoperability, and thus the need to separate and quantify XJ becomes increasingly important.

Most XJ studies for high-speed serial links took place in the context of multiple-lane serial channels [7],[8]. With the crosstalk quantified in terms of S-parameters, and using the linear system theory for channel signaling, simulating XJ for multiple-lane channel link is a relatively straightforward task. However, separating XJ under general signaling conditions, without the pre-knowledge of crosstalk S-parameters, and in the presence of other signal impairments and jitter components, is a much more complicated and difficult problem. Yet the knowledge and solution for this problem brings tremendous value to XJ quantification, debug, and diagnostics, as well as filling the solution gap of the overall jitter-separation method completion.

In view of unavailable technical publications on XJ separation methods and solutions, as well as its importance for designing and verifying a high-speed link at higher data rates, we dedicate this paper on XJ separation. In Section 1, we give a general introduction on the basics of crosstalk and its conversion mechanism to jitter. In Section 2, we focus on the correlated XJ (CXJ) separation, while Section 3 focuses on the uncorrelated XJ (UXJ) separation. Section 4 is dedicated to the validations of the new XJ separation methods and algorithms with experiments. Section 5 gives the summary and conclusion.

2. Crosstalk and Jitter Relationships

In this section, we first review the fundamentals for crosstalk, then discuss the crosstalk and jitter conversion relationship under two distinct conditions.

2.1 Crosstalk-Generation Mechanisms

The fundamental mechanisms for crosstalk are well studied and understood. Two basic coupling mechanisms produce crosstalk: the mutual capacitive coupling and the mutual inductive coupling. Figure 2 shows both inductive and capacitive coupling between two transmitting and receiving channels.

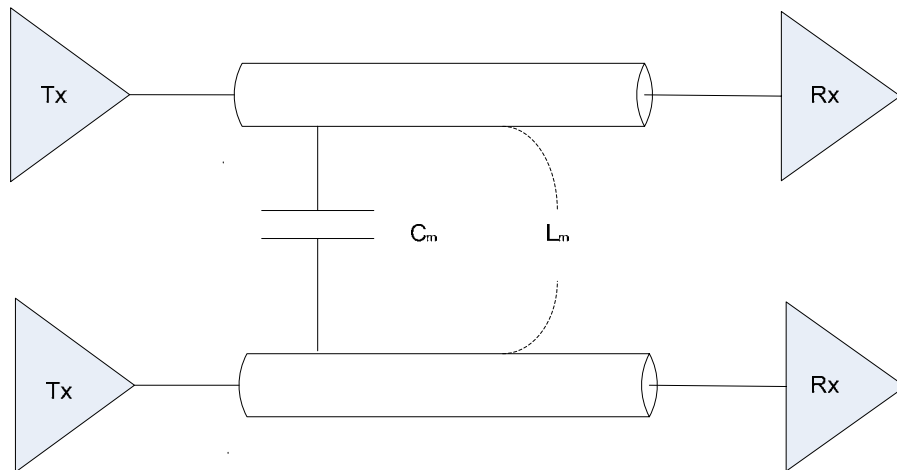


Figure 2. Inductive and capacitive crosstalk coupling

As illustrated, let us further assume that the top channel is the aggressor and the bottom channel is the victim. Using this assumption, the crosstalk-induced voltage noise due to the aggressor can be estimated. The inductive coupling-induced crosstalk voltage noise (ΔV_{mL}) is estimated as:

$$\Delta V_{mL} = L_m \frac{dI_a}{dt} = \frac{L_m}{Z_a} \frac{dV_a}{dt} \quad (1)$$

where L_m is the mutual inductive coefficient, Z_a is the impedance of the aggressor, and (dI_a / dt) and (dV_a / dt) are the current and voltage time derivatives for the aggressor.

The capacitive-coupling crosstalk voltage noise (ΔV_{mC}) is estimated as:

$$\Delta V_{mC} = C_m Z_v \frac{dV_a}{dt} \quad (2)$$

where C_m is the mutual capacitive coefficient, Z_v is the impedance of the victim, and (dV_a / dt) is the voltage time-change rate for the aggressor.

Equations (1) and (2) indicate that crosstalk-induced noise is proportional to the voltage time-change rate of the aggressor [5]. For a digital signal, the crosstalk-induced noise only occurs when there is a voltage time change, namely during the edge transition.

2.2 Correlated and Uncorrelated Crosstalk and jitter

In serial data communication, there are two common signal transmission modes. In the first, all channels transmit data synchronously or correlatedly, as in the case of a multiple-lane signal transmission in channel bonding mode for the same communication protocol (e.g., PCI Express, Fibre Channel). In the other, all channels transmit data independently or asynchronously. Many possible scenarios give rise to uncorrelated and asynchronous crosstalk, such as non-channel bonding multiple-lane operation for a same protocol link, and multiple-lane operation for multiple protocols. The jitter or voltage conversions for these two types of crosstalk are different and distinct.

2.2.1 Correlated Crosstalk-Induced Jitter

A multiple-lane operation link is shown in Figure 3. For illustration purposes, we only show a 3-lane link, however the concept can be extended to a N-lane link. For synchronous and correlated operation, all the data bit cell (voltage flat or non-edge transition period) and edge transitions are aligned. In this example, the center channel (channel 2) is the victim lane, the top (channel 1) and bottom (channel 3) channels are the aggressor lanes, and it uses a single-edge transition.

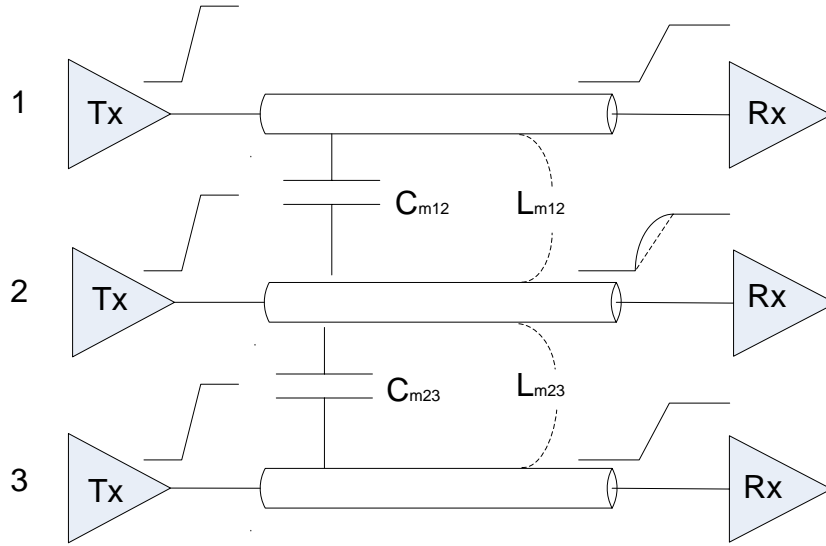


Figure 3. Synchronous and correlated crosstalk and its effect to the victim-lane edge transition

In this specific example, crosstalk-induced voltage noise adds to the victim-lane edge transition synchronously at the receiver side, assuming that the channel-to-channel skew and propagation delay difference are negligible. Based on Equations (1) and (2), the edge transitions of the victim lane are distorted. If the channel is lossless, then this synchronous time deviation or jitter at the 50% step response level is caused solely by the synchronous crosstalk. Since the aggressor edge transitions are synchronous with the victim edge transition, they are also synchronous in-phase. As such, the crosstalk-induced jitter manifests as a sub-component of the overall correlated jitter (experimentally shown in [9]). Consequently, it is possible to separate it from the rest of correlated jitter components using the detailed method and algorithm shown in Section 3.

2.2.2 Uncorrelated Crosstalk-Induced Jitter

As shown in Figure 3, if the aggressor channels and victim channel operate asynchronously or uncorrelatedly, then the phase relationship between aggressor and victim edge transitions are phase independent or random. Aggressor edge transitions may arrive during the bit period of the victim signal and the crosstalk produced by the aggressor edge transition only affects the voltage noise of the victim, not the timing jitter. If, however, aggressor edge transitions arrive during the edge transition of the victim, then the crosstalk for the aggressor edge transition only affects the edge transition and timing of the victim. If we further assume that the channel is ideal and lossless, and that the aggressor data pattern is random and has a reasonable number of edge transitions (e.g., PRBS $2^{12}-1$ has ~ 1000 edge transitions), then the central-limiting theorem effect becomes evident [5]. In this case, the crosstalk-induced jitter is best modeled or described by a truncated Gaussian [5], [10], [11]. This character or signature is the basis for separating asynchronous and uncorrelated crosstalk jitter from the rest of the jitter components.

3. Crosstalk-Induced Jitter Separation

Using the fundamental knowledge on correlated and synchronous crosstalk and uncorrelated and asynchronous crosstalk discussed in Section 2, we are ready to present the methods and algorithms for separating CXJ and UXJ from the rest of the jitter components.

3.1 Correlated-Crosstalk Jitter (CXJ) Separation

By definition, CXJ is correlated and synchronous with victim-lane signal edge transitions. As previously mentioned, CXJ is produced when one or multiple aggressors run with the same data rate and same data pattern synchronously and correlatedly with the victim lane, as in the case of a synchronous and correlated serial multiple-lane link operation. For discussion and mathematical-notation convenience, we assume that the signal waveform (i.e., $v_o(t)$ or voltage as a function of time) information for the victim-lane signal at the receiver side is readily available, with no record-length and/or resolution limitations relative to the application. The separation method then is:

Step 1: Apply the average (with significant enough statistics) to $v_o(t)$, then remove all uncorrelated jitter and noise, resulting in the correlated waveform ($v_{ave}(t)$) and the associated correlated jitter $\Delta t_{corr}(t_i)$ at the zero crossing or 50% level.

Step 2: Fit the correlated waveform with the intrinsic data-dependent waveform ($v_{ddw}(t)$) that follows the linear time-invariant (LTI) plus edge shifting rules to obtain the best parameters with the low-frequency-constrained data points in the correlated waveform. Using the obtained $v_{ddw}(t)$, DDJ ($\Delta t_{DDJ}(t_i)$) is estimated at the zero crossing or 50% level.

Step 3: Subtract the correlated jitter with the DDJ on a per-edge transition basis, which gives rise to the CXJ time record, namely $\Delta t_{CXJ}(t_i) = \Delta t_{corr}(t_i) - \Delta t_{DDJ}(t_i)$. The histogram or PDF for $\Delta t_{CXJ}(t_i)$ is then constructed, and statistical parameters, such as peak-to-peak (pk-pk) and rms values, are estimated.

3.2 Uncorrelated-Crosstalk Jitter (UXJ) Separation

As discussed in Section 2, UXJ is caused by aggressors running with their phases uncorrelated with the victim-lane signal. Again, we assume that the waveform of the victim-lane signal on the receiver side is readily available (i.e., $v_o(t)$ or voltage as a function of time). The separation method is as follows:

Step 1: Estimate the overall timing jitter ($\Delta t(t_i)$) or time interval error (TIE [3], [5]) based on $v_o(t)$ on a per-edge transition basis.

Step 2: Estimate the correlated jitter ($\Delta t_{corr}(t_i)$) from the averaged waveform $v_{ave}(t)$, then subtract it from the overall timing jitter $\Delta t(t_i)$ to get the uncorrelated jitter $\Delta t_{uc}(t_i)$ time record, namely $\Delta t_{uc}(t_i) = \Delta t(t_i) - \Delta t_{corr}(t_i)$.

Step 3: Build the uncorrelated jitter histogram or PDF from the uncorrelated jitter $\Delta t_{uc}(t_i)$ time record, and calculate the corresponding BER CDF via integration from the histogram or PDF.

Step 4: Fit the uncorrelated jitter histogram or PDF with a Gaussian (to account for RJ) combined with a truncated Gaussian (to account for uncorrelated UXJ). The best-fitted truncated Gaussian provides both pk-pk and rms values for the uncorrelated UXJ, and the best-fitted Gaussian provides the rms values for intrinsic RJ. Alternatively, an uncorrelated BER CDF can be fitted with an integrated Gaussian combined with an integrated truncated Gaussian. The best-fitted integrated truncated Gaussian gives both pk-pk and rms values for the uncorrelated UXJ, and the best-fitted Gaussian provides the rms values for intrinsic RJ.

Note that uncorrelated jitter $\Delta t_{ucorr}(t_i)$ -corresponded PDF has both intrinsic RJ and UXJ components. It is well known that the RJ PDF is best modeled by a Gaussian, and, as we discussed in Section 2, UXJ is best modeled by a truncated Gaussian. Therefore, the PDF model is represented as:

$$f_{UC}(\Delta t) = f_{RJ}(\Delta t) \otimes f_{UXJ}(\Delta t) \quad (3)$$

where $f_{UC}(\Delta t)$ is the overall PDF for uncorrelated jitter, $f_{RJ}(\Delta t)$ is the PDF for RJ, $f_{UXJ}(\Delta t)$ is the PDF for UXJ, and \otimes denotes the convolution. $f_{RJ}(\Delta t)$ is Gaussian and is described by the following equation:

$$f_{RJ}(\Delta t) = \frac{1}{\sqrt{2\pi}\sigma_{RJ}} e^{-\frac{\Delta t^2}{2\sigma_{RJ}^2}} \quad (4)$$

where σ_{RJ} is the sigma or rms value of Gaussian. $f_{UXJ}(\Delta t)$ is described as

$$f_{UXJ}(\Delta t) = \begin{cases} \frac{1}{\sqrt{2\pi}\sigma_{UXJ}} e^{-\frac{\Delta t^2}{2\sigma_{UXJ}^2}} & \text{for } |\Delta t| \leq UXJ_{pk} \\ 0 & \text{for } |\Delta t| > UXJ_{pk} \end{cases} \quad (5)$$

where σ_{UXJ} is the sigma value, and UXJ_{pk} is the peak value for UXJ.

Two different types of asymptotic behavior for $f_{UXJ}(\Delta t)$ can be obtained. In the high-probability region when $|\Delta t| \ll UXJ_{pk}$, f_{UXJ} is the convolution of two Gaussians and the result is still a Gaussian with a rms value $\sigma_{UXJ} \rightarrow \sqrt{\sigma_{UXJ}^2 + \sigma_{RJ}^2}$. However, in the low-probability

region where $|\Delta t| \gg UXJ_{pk}$, f_{UJ} approaches f_{RJ} and $\sigma_{UJ} \rightarrow \sigma_{RJ}$. An illustration of f_{UJ} is shown in Figure 4.

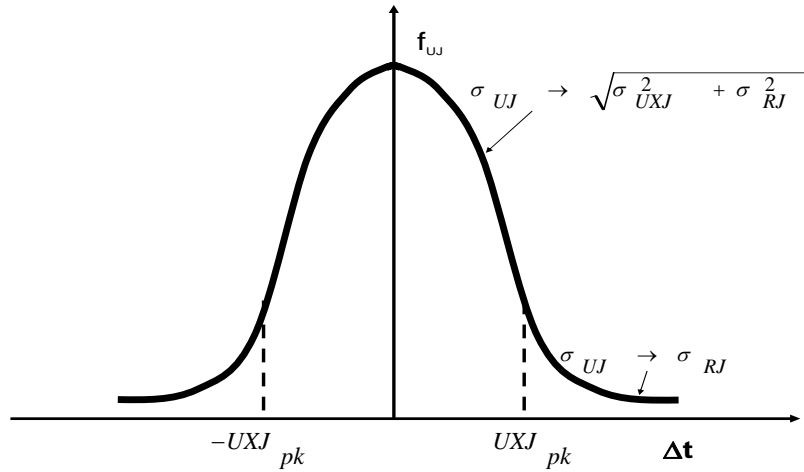


Figure 4. An uncorrelated jitter PDF composed of UXJ and RJ

4. Experimental Validation

To prove the validity of the proposed methods for separating correlated and uncorrelated crosstalk jitter, a well-defined experiment with good controllability is needed so that the conditions for the methods to work can be met. The experimental diagram shown in Figure 5 creates CXJ and UXJ.

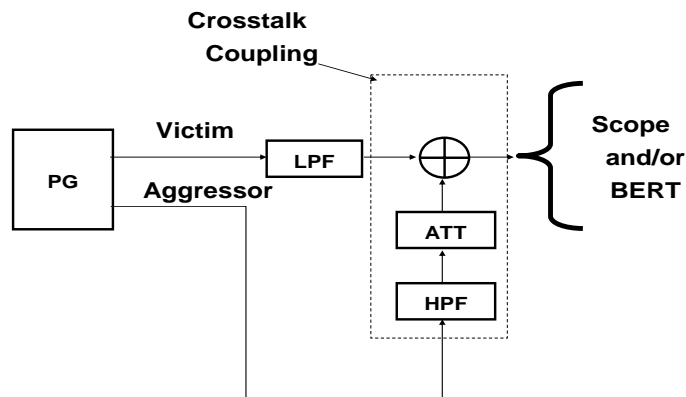


Figure 5. An experimental setup for generating CXJ and UXJ

In this experimental setup, the aggressor and victim signals are created by a multiple-channel pattern generator (PG). The victim signal goes through a low-pass filter (LPF) to slow down the slow-rate of edge transitions of the data pattern and enabling amplitude modulation. The aggressor signal runs synchronously with the victim signal to generate CXJ and UXJ. The inductive and capacitive coupling is emulated with a high-pass filter (HPF, for time derivative emulation), an ATT (attenuation, for coupling level), and a signal combiner (for amplitude modulation).

4.1 CXJ Generation and Separation

To create CXJ, the victim and the aggressor must be in-phase and operating with same data-pattern and data rate. We chose the PRBS $2^{10}-1$ data pattern and the 3-Gbps data rate for both victim and aggressor in this example experiment. Using the method and algorithm described in Section 3.1, we obtained the overall correlated jitter time record $\Delta t_{corr}(t_i)$, the DDJ record $\Delta t_{DDJ}(t_i)$, and the CXJ record $\Delta t_{CXJ}(t_i)$, as shown in Figure 6.

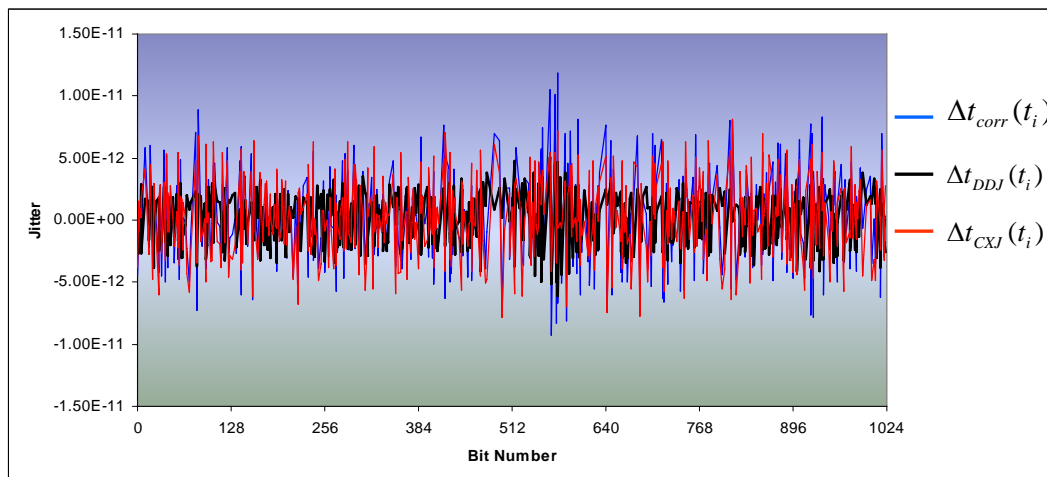


Figure 6. Overall correlated jitter, DDJ, and CXJ time records

The corresponding histograms can be calculated based on the data shown in Figure 6, and the results are shown in Figure 7.

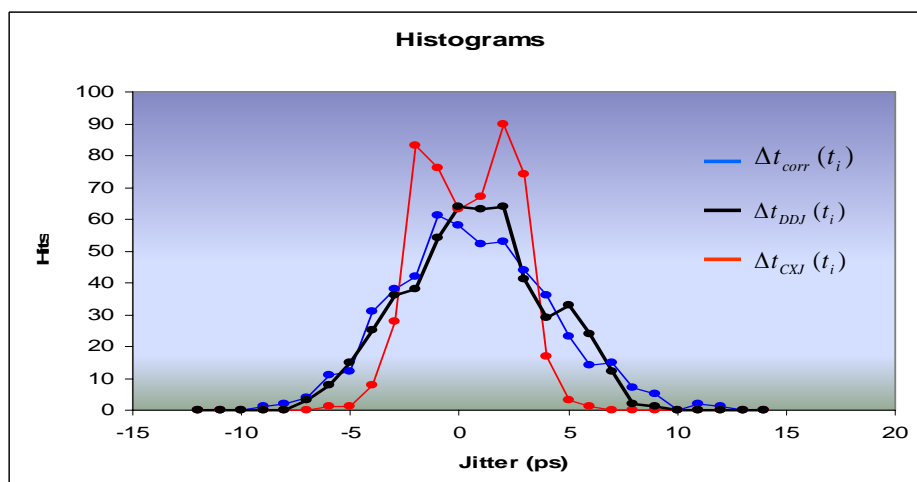


Figure 7. Overall correlated jitter, DDJ, and CXJ histograms

Using this histogram, the statistical parameters can be calculated, as shown in Table 1.

Table 1: Statistical Parameters for Correlated jitter, DDJ, and CXJ

	$\Delta t_{corr}(t_i)$	$\Delta t_{DDJ}(t_i)$	$\Delta t_{CXJ}(t_i)$
Stdev (ps)	3.50	2.100	3.18
Max (ps)	11.80	5.02	8.10
Min (ps)	-9.29	-6.10	-7.85
Pk-pk (ps)	21.09	11.12	15.95

4.2 UXJ Generation and Separation

To create UXJ, the victim and aggressor must be phase independent or random, which is achieved by running different data patterns for victim and aggressor lanes. We chose the PRBS $2^{10}-1$ data pattern for the victim, and PRBS $2^{31}-1$ for the aggressor, with both running at 3 Gbps. Using the method and algorithm described in Section 3.2, we obtained an uncorrelated BER CDF in Q-space [5], [10], [11] and the corresponding fitting, as shown in Figure 8.

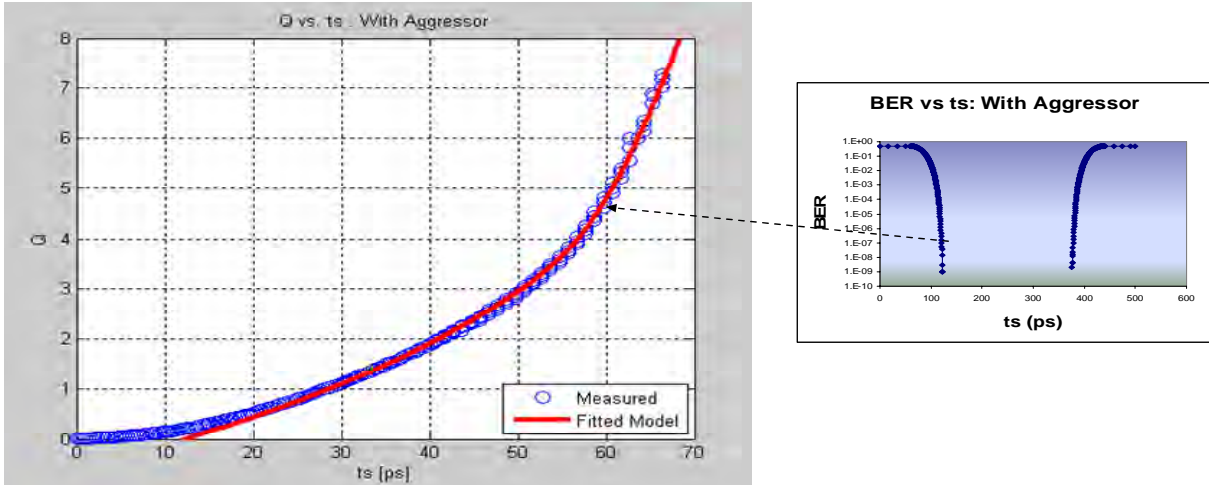


Figure 8. BER CDF (right), BER CDF in Q-space (left) for the left branch with fitting

The integration of Equation (3) is used to fit the BER CDF in Q-space, and yields sigma and rms values for UXJ and a true intrinsic RJ. We found $\sigma_{UXJ} = 26.50$ ps, $UXJ_{pk} = 48.76$ ps, (i.e., crest factor = 0.92), and $\sigma_{RJ} = 1.83$ ps. We assume that the left and right branches of the BER CDF are symmetrical.

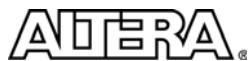
5. Summary

New crosstalk jitter (XJ) separation methods and algorithms that separate crosstalk jitter from the rest of the jitter components are presented in this paper. Separating crosstalk jitter from the rest of the jitter components has been a standing challenge for years, but now it has a proven and verified solution. The described methods and algorithms classify XJ into two types, correlated crosstalk jitter (CXJ) and uncorrelated crosstalk jitter (UXJ), and separate them according to their distinct characteristics. Specifically, CXJ is separated by subtracting the DDJ from the total

correlated jitter. In contrast, UXJ is separated by fitting the jitter PDF with an unbounded uncorrelated Gaussian (i.e., manifesting the true random jitter process) combined with an bounded uncorrelated Gaussian (i.e., manifesting the UXJ process), or by fitting the BER CDF with an integrated unbounded uncorrelated Gaussian combined with an bounded uncorrelated Gaussian, in either linear or Q-space. The feasibility of this new crosstalk jitter separation is further demonstrated and proven with controlled experiments.

References

- [1] J. Wilstrup, "A Method of Serial Data Jitter Analysis Using One-Shot Time Interval Measurements," IEEE/ITC, 1998.
- [2] M. Li, J. Wilstrup, R. Jessen, D. Petrich, "A New Method for Jitter Decomposition Through its Distribution Tail Fitting," IEEE/ITC, 1999.
- [3] B. Ward, K. Tan, M. Guenther, "Apparatus and Method for Spectrum Analysis-Based Serial Data Jitter Measurement," U.S. Patent 6,832,172, 2004.
- [4] N. Buren, M. Chura, G. LeCheminant, J. Stimple, M. Viss, "Jitter Separation at Data Rates Above 3 Gb/s," DesignCon, 2004.
- [5] M. Li, *Jitter, Noise, and Signal Integrity at High-Speed*, Prentice Hall, ISBN 0132429616, 2007.
- [6] American National Standard Institutes (ANSI) and National Committee for Information Technology Standardization (NCITS), "Fibre Channel-Methodologies for Jitter and Signal Quality Specification – MJSQ," Rev 14, 2004.
- [7] J. Buckwalter, B. Analui, A. Hajimiri, "Data-Dependent Jitter and Crosstalk-Induced Bounded Uncorrelated Jitter in Copper Interconnects," IEEE Microwave Symposium Digest, 2004.
- [8] A. Kuo, T. Farahmand, N. Ou, S. Tabatabaei, and A. Ivanov, "Jitter Models and Measurement Methods for High-Speed Serial Interconnects," IEEE/ITC, 2004.
- [9] D. Chow, "Analysis of Crosstalk Effects on Jitter in FPGA Transceivers," DesignCon, 2008.
- [10] M. Shimanouchi, M. Li, and D. Chow, "New Modeling Methods for Bounded Gaussian Jitter (BGJ)/Noise (BGN) and Their Applications in Jitter/Noise Estimation/Testing," IEEE/ITC, 2009.
- [11] M. Li, "A New Jitter Classification Method Based on Statistical, Physical, and Spectroscopic Mechanisms," IEC/DesignCon 2009.



101 Innovation Drive
San Jose, CA 95134
www.altera.com

Copyright © 2010 Altera Corporation. All rights reserved. Altera, The Programmable Solutions Company, the stylized Altera logo, specific device designations, and all other words and logos that are identified as trademarks and/or service marks are, unless noted otherwise, the trademarks and service marks of Altera Corporation in the U.S. and other countries. All other product or service names are the property of their respective holders. Altera products are protected under numerous U.S. and foreign patents and pending applications, maskwork rights, and copyrights. Altera warrants performance of its semiconductor products to current specifications in accordance with Altera's standard warranty, but reserves the right to make changes to any products and services at any time without notice. Altera assumes no responsibility or liability arising out of the application or use of any information, product, or service described herein except as expressly agreed to in writing by Altera Corporation. Altera customers are advised to obtain the latest version of device specifications before relying on any published information and before placing orders for products or services.